Synthesis and Structure Solution of Zeolite SSZ-65

Saleh Elomari, Allen W. Burton,* Kenneth Ong, Ajit R. Pradhan, and Ignatius Y. Chan

Chevron Energy Technology Company, 100 Chevron Way, Richmond, California 94802

Received February 15, 2007. Revised Manuscript Received August 21, 2007

This report describes the synthesis and structure solution of the new zeolite SSZ-65. SSZ-65 may be prepared as either a borosilicate ($Si_{52.5}B_{1.5}O_{108}$) or an aluminosilicate using 1-[1-(4-chloro-phenyl)-cyclopropylmethyl]-1-ethyl-pyrrolidinium as a structure-directing agent. The structure of SSZ-65 was determined with the FOCUS Fourier recycling method. The framework of SSZ-65 possesses a two-dimensional system of intersecting 12-ring channels with pore apertures of 6.9 Å × 5.9 Å. The topological symmetry of SSZ-65 is *P*6/*mmm*, but improvements in the Rietveld refinement of the powder diffraction data are obtained in space group *P*6/*m* (a = 16.8009(2) Å and c = 12.6154(1) Å). The agreement values improve from R_{wp} = 0.116, R_p = 0.094, and $R(F^2)$ = 0.142 in *P*6/*mmm* to R_{wp} = 0.103, R_p = 0.085, and $R(F^2)$ = 0.092 in *P*6/*m*.

Introduction

Organic structure-directing agents (SDAs) often play a central role in the discovery of high-silica zeolites with novel framework topologies. The earliest reports of the inclusion of organic molecules in zeolite gel mixtures include the work by Barrer and Denny,[1] Aiello and Barrer,[2] and Kerr.[3] These studies examined the syntheses of zeolites using tetramethylammonium (TMA) cations (Figure 1) in conjunction with alkali metal hydroxides. The crystal structures of the products were topologically equivalent with previously reported zeolites (LTA, SOD), but they were more silica-rich (Si/Al = 3−5) than their counterparts synthesized only in the presence of metal cations (Si/Al ∼ 1). Because bulky organic cations occupy more space than metal cations and therefore fewer cations are occluded within the zeolite structure, it was soon recognized that zeolites with occluded TMA cations must possess a lower aluminum concentration for charge compensation of the extraframework cations. A later realization was that using even larger alkylammonium ions in zeolite synthesis may not only produce zeolites with higher Si/Al ratios but may also lead to high-silica materials with previously unseen pore architectures. Workers at Mobil began using large (C/N > 7) quaternary ammonium cations in their synthesis mixtures during the late 1960s. Zeolites β (BEA*)[4] and ZSM-12[5] (**MTW**), ZSM-5[6] (**MFI**), and ZSM-11[7] (**MEL**) resulted from the use of tetraethylammonium, tetrapropylammonium (TPA), and tetrabutylammonium (TBA) cations, respectively (see Figure 1). The branched structures of the TPA and TBA cations are reflected in the multidimensional systems of medium pores that ZSM-5 and ZSM-11 possess.

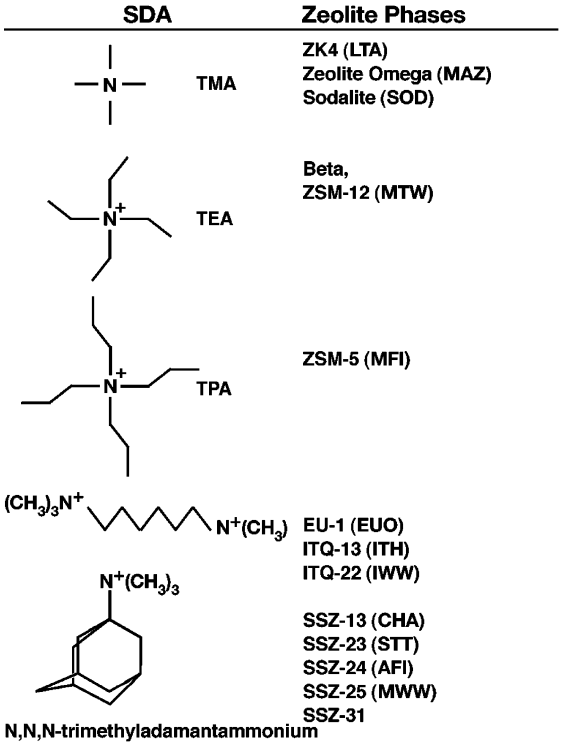

Figure 1. Organic SDA molecules used in early zeolite syntheses and examples of zeolite phases that have been prepared with them.

Early on, the term "template" was (and still is) frequently applied to describe the role of the organic species in the zeolite formation. However, a single SDA molecule may direct the formation of several different zeolite structures and some zeolite structures may be formed in the presence of several different organic molecules. Lobo and Davis therefore later used the term "structure-directing agent" to describe the organic molecule.[8] This term signifies a strong influence of the organic molecule on the phase selectivity, but it does not imply a uniqueness that is often associated with the term "template."

* Corresponding author. E-mail: buaw@chevron.com. Phone: 510-242-1810. Fax: 510-242-1792.

(1) Barrer, R. M.; Denny, P. J. *J. Chem. Soc.* **1961**, 983.
(2) Aiello, R.; Barrer, R. M. *J. Chem. Soc. A* **1970**, 1470.
(3) Kerr, G. T. *Inorg. Chem.* **1966**, *5*, 1537.
(4) Wadlinger, R. L.; Kerr, G. T.; Roskinski, E. J. U.S. Patent 3308069, 1967.
(5) Rosinski, E. J.; Rubin, M. K. U.S. Patent 3832449, 1974.
(6) Argauer, R. J.; Landolt, G. R. U.S. Patent 3702886, 1972.
(7) Chu, P. U.S. Patent 3709979, 1973.
(8) Lobo, R.; Davis, M. *Chem. Mater.* **1992**, *22*, 1665.

10.1021/cm070459t CCC: $37.00
Published on Web 10/12/2007

Since the pioneering Mobil studies, high-silica syntheses with other alkylamines or alkylammonium cations have resulted in a large number of zeolites with novel framework topologies or in materials with known framework structures but previously undiscovered compositional ranges. A comprehensive database of zeotype frameworks may be examined at the IZA webpage at http://www.iza-structure.org/databases/.[9] Early on, many organic SDAs were either readily available from chemical suppliers, or they were easily prepared from single-step alkylation reactions of an available amine with an appropriate alkyl halide. In many cases, the same SDA was used to prepare more than one previously undiscovered phase by varying the inorganic gel conditions. For example, Zones and co-workers used the methylated derivative of 1-adamantamine (*N*,*N*,*N*-trimethyl-adamantammonium—Figure 1) to prepare zeolites SSZ-13 (**CHA**), SSZ-23 (**STT**), SSZ-24 (**AFI**), and SSZ-25 (**MWW**).[10,11] Later Gittleman et al. used this same molecule to prepare SSZ-31.[12] Researchers also examined diquaternary ammonium molecules formed by reaction of α,ω-dihaloalkanes with a tertiary amine. Use of these diquaternary molecules has led to the discoveries of several zeolites including EU-1 (**EUO**),[13−17] ZSM-57 (**MFS**),[18] Nu-87 (**NES**),[19] Nu-86,[20] SSZ-16 (**AFX**),[21] IM-5[22] (**IMF**), ITQ-13 (**ITH**),[23] ITQ-22 (**IWW**),[24,25] and TNU-9 (**TUN**).[26]

Several groups have recently utilized more sophisticated reaction schemes to prepare precursor amines which are currently unavailable from commercial suppliers. For example, Nakagawa and co-workers synthesized polycyclic SDA molecules derived from products of Diels−Alder, Mannich, or Michael addition reactions.[27] These SDA produced the novel zeolites SSZ-35 (**STF**), SSZ-36 (**ITE**/**RTH**), and SSZ-39 (**AEI**). Other notable examples include the SDA for the recently reported zeolites MCM-68[28] and ITQ-32 (**ITW**).[29] The SDA for MCM-68 (**MSE**) is formed from a diimide derived from a Diels−Alder adduct, and one of the SDA for ITQ-32 is produced from a diimide derived from the photocatalyzed [2 + 2] cycloaddition reaction of *N*-methylmaleimide.

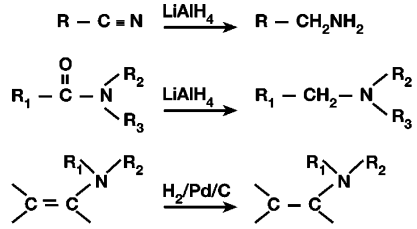

Figure 2. Methods to prepare amines.

After the Nakagawa studies, we continued to explore bulky, rigid SDA molecules derived from Diels−Alder reactions. Many of these molecules remained selective for SSZ-35 or SSZ-36, and we were unable to discover any novel phases within the inorganic conditions we examined. We later examined more flexible quaternary ammonium molecules. The precursor amines were prepared by reduction of amides (or lactams), enamines,[30] or nitriles[31] (see Figure 2). The SDA often possessed one or more (unfused) ring structures. These SDAs have resulted in several new zeolites including SSZ-53[32] (**SFH**), SSZ-55 (**ATS**),[33] SSZ-57,[34] SSZ-58[35] (**SFG**), SSZ-59[32] (**SFN**), SSZ-60[36] (**SSY**), SSZ-63,[37] SSZ-64,[38] and SSZ-65. Here we report the synthesis and structure determination of SSZ-65, a zeolite with an unusual structure.

Experimental Section

Synthesis of Structure-Directing Agent. The SDA for SSZ-65, 1-[1-(4-chloro-phenyl)-cyclopropylmethyl]-1-ethyl-pyrrolidinium, is prepared[39] according to the scheme presented in Figure 3. Note that the nonchlorinated analogue 1-ethyl-1-(1-phenyl-cyclopropylmethyl)-pyrrolidinium also may be used to prepare SSZ-65. In the first step, the parent amide is prepared by the reaction of pyrrolidine with 1-(4-chloro-phenyl)-cyclopropanecarbonyl chloride. A 2 L round-bottomed flask equipped with a mechanical stirrer is charged with 1000 mL of dry benzene, 53.5 g (0.75 mol) of pyrrolidine, and 76 g (0.75 mol) of triethylamine. The flask is then cooled to 0 °C in an ice−water bath. Next a solution is prepared by mixing 108 g of 1-(4-chloro-phenyl)-cyclopropanecarbonyl chloride (0.50 mol) with 100 mL of benzene. This solution is then added dropwise to the cooled amine solution. After the addition is completed, the mixture is allowed to stir overnight at room

(9) Baerlocher, Ch.; McCusker, L. *Database of Zeolite Structures.* http://www.iza-structure.org/databases/ (accessed March 21, 2007).
(10) Zones, S. I.; Van Nordstrand, R. A.; Santilli, D. S.; Wilson, D. M.; Yuen, L.; Scampavia, L. D. *Zeolites: Facts, Figures, Future*; Jacobs, P. A., van Santen, R. A., Eds.; Studies in Surface Science and Catalysis 49A; Elsevier: Amsterdam, 1989; pp 299−309.
(11) Nakagawa, Y.; Lee, G. S.; Harris, T. V.; Yuen, L. T.; Zones, S. I. *Microporous Mesoporous Mater.* **1998**, *22*, 69−85.
(12) Gittleman, C.; Bell, A.; Radke, C. *Catal. Lett.* **1996**, *38*, 1−9.
(13) Casci, J. L.; Lowe, B. M.; Whitam, T. V. Eur. Pat. Appl. 42226, 1981.
(14) New Developments in Zeolite Science and Technology, Aug 17−22, 1986; Murakami, Y., Iijima, A., Ward, J. W., Eds.; Elsevier: Tokyo, 1986; p 215.
(15) Proceedings of the Sixth International Zeolite Conference, July 10−15, 1983, Reno, NV; Olson, D., Bisio, A., Eds.; Butterworths: Guildford, U.K., 1983; p 894.
(16) Dodwell, G. W.; Denkewicz, R. P.; Sand, L. B. *Zeolites* **1985**, *5*, 153.
(17) Rao, G. N.; Joshi, P. N.; Kotasthane, A. N.; Ratnasamy, P. *Zeolites* **1983**, *9*, 483−490.
(18) Valyocsik, E. W.; Page, N. M. (Mobil Oil Corporation) Eur. Patent 0 174 121 A2, 1985.
(19) Casci, J. L.; Stewart, A. (ICI plc) Eur. Pat. Appl. 377 291, 1990.
(20) Casci, J. L. U.S. Patent 5,108,579, 1992.
(21) Lobo, R. F.; Zones, S. I.; Medrud, R. *Chem. Mater.* **1996**, *8*, 2409.
(22) Benazzi, E.; Guth, J.-L.; Rouleau, L. WO Patent 9817581, 1998.
(23) Corma, A.; Puche, M.; Rey, F.; Sankar, G.; Teat, S. J. *Angew. Chem., Int. Ed.* **2003**, *42*, 1156.
(24) Corma, A.; Rey, F.; Valencia, S.; Jordá, J. L.; Rius, J. *Nat. Mater.* **2003**, *2*, 493−497.
(25) Sastre, G.; Pulido, A.; Castaneda, R.; Corma, A. *J. Phys. Chem. B* **2004**, *108* (26), 8830−8835.
(26) Gramm, F.; Baerlocher, Ch.; McCusker, L. B.; Warrender, S. J.; Wright, P. A.; Han, B.; Hong, S. B.; Liu, Z.; Ohsuna, T.; Terasaki, O. *Nature* **2006**, *444*, 79−81.
(27) Wagner, P.; Nakagawa, Y.; Lee, G. S.; Davis, M. E.; Elomari, S.; Medrud, R. C.; Zones, S. I. *J. Am. Chem. Soc.* **2000**, *122* (2), 263−273.
(28) Dorset, D. L.; Weston, S. C.; Dhingra, S. S. *J. Phys. Chem. B* **2006**, *110* (5), 2045−2050.
(29) Cantin, A.; Corma, A.; Leiva, S.; Rey, F.; Rius, J.; Valencia, S. *J. Am. Chem. Soc.* **2005**, *127* (33), 11560−11561.
(30) Elomari, S. U.S. Patent 6616911, 2003.
(31) Elomari, S. U.S. Patent 6632417, 2003.
(32) Burton, A.; Elomari, S.; Chen, C. Y.; Medrud, R. C.; Chan, I. Y.; Bull, L. M.; Kibby, C.; Harris, T. V.; Zones, S. I.; Vittoratos, E. S. *Chem. Eur. J.* **2003**, *9*, 5737−5748.
(33) Wu, M. G.; Deem, M. W.; Elomari, S. A.; Medrud, R. C.; Zones, S. I.; Maesen, T.; Kibby, C.; Chen, C.-Y.; Chen, I. Y. *J. Phys. Chem. B* **2002**, *106*, 264−270.
(34) Elomari, S. U.S. Patent 6544495, 2003.
(35) Burton, A.; Elomari, S.; Medrud, R. C.; Chan, I. Y.; Chen, C.-Y.; Bull, L. M.; Vittoratos, E. S. *J. Am. Chem. Soc.* **2003**, *125*, 1633−1642.
(36) Burton, A.; Elomari, S. *Chem. Commun.* **2004**, 2618−1619.
(37) Burton, A. W.; Elomari, S.; Chan, I.; Pradhan, A.; Kibby, C. *J. Phys. Chem. B* **2005**, *109* (43), 20266−20275.
(38) Elomari, S. U.S. Patent 6569401, 2003.
(39) Elomari, S. U.S. Patent 7011811, 2006.

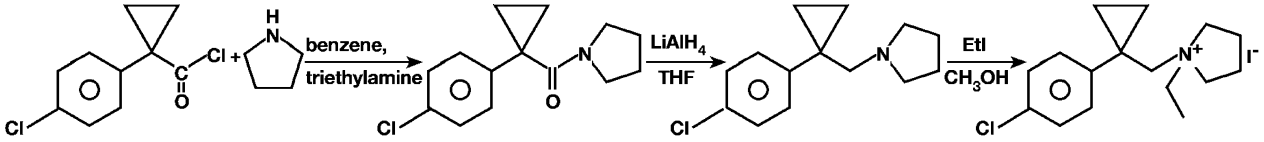

Figure 3. Reaction scheme to prepare SDA for zeolite SSZ-65.

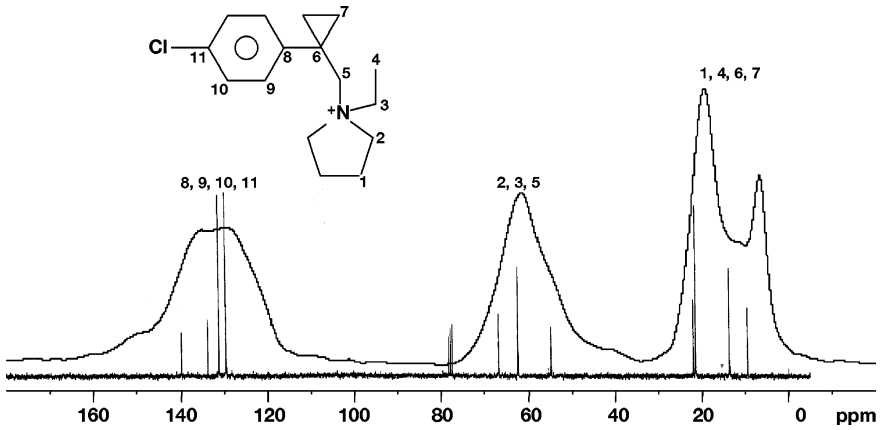

Figure 4. $^{1}H-^{13}C$ CP liquid NMR spectrum of 1-[1-(4-chloro-phenyl)-cyclopropylmethyl]-1-ethyl-pyrrolidinium in deuterated chloroform (bottom trace) and the $^{1}H-^{13}C$ CP MAS solid-state NMR spectrum of the as-made form of SSZ-65.

temperature. The resulting biphasic mixture (a liquid and tan-colored precipitate) is concentrated on a rotary evaporator to remove the solvent and excess pyrrolidine. The remaining residue is diluted with 750 mL of water and then extracted with chloroform. The organic layer is washed twice with 500 mL of water and once with brine. Anhydrous sodium sulfate is then mixed with the chloroform solution to remove residual water, the salt is then removed by filtration, and the chloroform is evaporated with a rotary evaporator to obtain 122 g of amide (0.49 mol, 97% yield) as a tan-colored solid.

In the next step, the amide is reduced to a tertiary amine. A three-necked 3 L reaction flask is equipped with a mechanical stirrer and a reflux condenser. The flask is cooled to 0 °C with an ice bath. A volume of 750 mL of anhydrous tetrahydrofuran (THF) and then 45.5 g of $LiAlH_4$ (1.2 mol) are added to the flask. A solution is then prepared by dissolving 120 g of the amide in 250 mL of THF. This solution is added dropwise to the LAH suspension (still at 0 °C). After complete addition of the amide solution, the ice bath is removed and replaced with a heating mantle, and the suspension is refluxed overnight. The heating mantle is then removed and replaced with an ice bath to cool the suspension to 0 °C. A volume of 500 mL of diethyl ether is then added to the mixture, and then 160 mL of a 15% (by mass) NaOH solution is added dropwise with vigorous stirring. After the starting gray mixture turns into a clear solution with a white powdery precipitate, the mixture is filtered to remove the inorganic solids. The filtrate is then mixed with anhydrous magnesium sulfate to dry the solution, the mixture is filtered to remove the salts, and the solution is concentrated on a rotary evaporator to yield 106 g of amine as a pale yellow, oily substance. ^{1}H and ^{13}C liquid NMR indicates the amine is pure within detectable limits.

In the final step, the amine is alkylated to obtain the desired quaternary ammonium molecule. In a three-necked 3 L reaction flask, 100 g (0.42 mol) of the amine is dissolved in 1000 mL of anhydrous methanol. An amount of 98 g of iodoethane (0.62 mol) is then added, and the mixture is stirred for 72 h. Next, 39 g (0.25 mol) of additional iodoethane is added, and the mixture is refluxed for 3 h. The solution is then cooled down, and the solvent and excess iodoethane are removed at reduced pressure in a rotary evaporator. The dark tan-colored product is then purified by dissolving it in 500 mL of acetone. Precipitation of the quaternary ammonium salt from solution with diethyl ether gave 153 g (93%) of the quaternary ammonium molecule as a white powder. The product is pure within detectable limits by ^{1}H and ^{13}C liquid NMR analysis (Figure 4).

The hydroxide form of the SDA is obtained by ion exchange of an aqueous solution of the iodide salt with at least a 2-fold excess of Biorad exchange resin (ion-exchange resin-OH, AH1-X8). The hydroxide concentration of the SDA solution is determined by titration with a 0.1 N HCl solution.

Zeolite Syntheses. The following procedure describes the synthesis of borosilicate SSZ-65. A 23 mL Teflon liner is charged with 5.4 g of 0.6 M aqueous solution of 1-[1-(4-chlorophenyl)-cyclopropylmethyl]-1-ethyl-pyrrolidinium hydroxide (3 mmol SDA), 1.2 g of 1 M aqueous solution of NaOH, and 5.4 g of deionized water. To this solution, 0.06 g of sodium borate decahydrate is added and stirred until completely dissolved. Then, 0.9 g of Cabosil M-5 fumed silica is added to the solution, and the mixture is thoroughly stirred to create a uniform suspension. The resulting gel is capped off and placed in a Parr bomb steel reactor and heated in an oven at 160 °C while rotating at 43 rpm. The reaction is monitored by periodically removing the reactor from the oven, checking the pH of the gel mixture, and looking for crystal formation using scanning electron microscopy (SEM). The reaction is usually complete after heating for 9−12 days at the conditions described above. After complete crystallization, the powdery product is filtered through a fritted-glass funnel. The collected solids are thoroughly washed with water and rinsed with acetone (10 mL) to remove any organic residues. The solids are allowed to air-dry overnight and are subsequently dried in an oven at 120 °C for 1 h. The reaction typically yields 0.85 g of solid product. When the synthesis is repeated in the presence of SSZ-65 seeds, only 4 days are required for crystallization of the product.

The aluminosilicate version of SSZ-65 may be prepared according to two different routes. The first route is a direct synthesis that uses zeolite Y as an aluminum source. In this case, 4 g of 0.6 M aqueous solution of 1-[1-(4-chlorophenyl)-cyclopropylmethyl]-1-ethyl-pyrrolidinium hydroxide (2.25 mmol SDA), 1.5 g of 1 M aqueous solution of NaOH (1.5 mmol NaOH), and 2 g of deionized water are added together in a 23 mL Teflon liner. To this solution, 0.25 g of Na−Y zeolite (LZY-52 from Union Carbide $SiO_2/Al_2O_3 = 5$) and 0.85 g of Cabosil M-5 are added to the solution, and the

mixture is thoroughly stirred. The mixture is then heated for about 16 days at 160 °C. The yield of solid product from the synthesis is 1.05 g. The product Si/Al ratio measured by inductively coupled plasma (ICP) methods is 17.2. Note that this ratio is consistent with the incorporation of nearly all the aluminum from the original gel. The second route involves a postsynthetic treatment of the calcined borosilicate with a concentrated aqueous solution of aluminum nitrate. This has previously been described by Chen and Zones[40] as a method to convert large-pore borosilicates to their analogous aluminosilicate forms. The treatment extracts boron from the zeolite framework and replaces the extracted boron with aluminum. In this procedure, 1.0 g of the calcined borosilicate is suspended in 15 mL of 1 M aluminum nitrate aqueous solution and heated at reflux overnight. The solids are then filtered and thoroughly rinsed with water to remove excess aluminum salt. Chemical analyses of the parent borosilicate (Si/B = 35) and the aluminosilicate indicate (Si/Al = 33) indicate a near stoichiometric replacement of boron by aluminum after the treatment. There is no detectable boron in the sample after the treatment.

Characterization Methods. Preliminary powder X-ray diffraction (XRD) patterns were recorded on a Siemens D-500 instrument. Diffraction peaks from the in-house diffraction data were profile-fitted and subsequently indexed with the MDI JADE software package. Scanning electron micrographs were recorded on a JEOL JSM-6700F instrument. Transmission electron micrographs (TEM) and electron diffraction patterns were obtained with a JEOL 2010 instrument operating at an accelerating voltage of 200 kV. Samples were prepared by dispersing the crystallites on a continuous carbon film. A calcined borosilicate sample for detailed structural analysis was examined at Beamline X16C at Brookhaven National Laboratory. The SDA was removed by calcination to 595 °C in an atmosphere of nitrogen containing 2% oxygen. The X16C sample was packed in a 1.5 mm outer diameter glass capillary that was sealed after being evacuated and heated overnight at 350 °C. Data were collected at ambient temperature with a scintillation detector from 4° to 60° 2θ in steps of 0.005° 2θ and a wavelength of 1.19958 Å. Data from 4° to 30° 2θ were collected for 2 s/step, and data from 30° to 60° 2θ were collected for 4 s/step. The starting model for the Rietveld structure refinement (performed with GSAS[41]) was generated with the FOCUS algorithm[42] using Cu Kα radiation. Initial distance−least-squares refinement of the framework found with the FOCUS method was carried out with DLS-76.[43] Chemical analyses for Si, B, Cl, C, N, and Na were performed by Galbraith Laboratories (Oak Ridge, Tennessee) by the ICP method. Thermogravimetric analyses (TGA) were performed by heating an as-made zeolite sample in air to 200 °C at 5 °C/min, holding the temperature at 200 °C for 2 h, and then heating to a final temperature of 800 °C at 5 °C/min. Micropore volumes were calculated from *t*-plot analyses of data for the nitrogen isotherms.[44]

The NMR spectra were recorded at room temperature on a Bruker AVANCE 500 wide-bore spectrometer operating at 125.7537 MHz for ^{13}C nuclei and 500.115 MHz for ^{1}H nuclei. The experiments were performed using a 4 mm triple-resonance Bruker magic-angle spinning (MAS) probe. The cross-polarization (CP) magic-angle spinning (MAS) spectrum was collected with cross-polarization from proton using a 90° pulse length of 3.6 μs and contact time of 3000 μs. A relaxation delay of 2 s was sufficient to complete relaxation. A total of 16 000 scans were acquired, and the sample was spun at the magic angle at 10 kHz. The data were processed with 250 Hz line broadening. The chemical shifts are given relative to tetramethylsilane at zero ppm and were referenced externally using adamantane as reference standard. For the NMR of liquid samples, tetramethylsilane was used as a internal standard. The tentative assignments of the spectrum are based on literature chemical shifts from molecules with similar chemical groups.

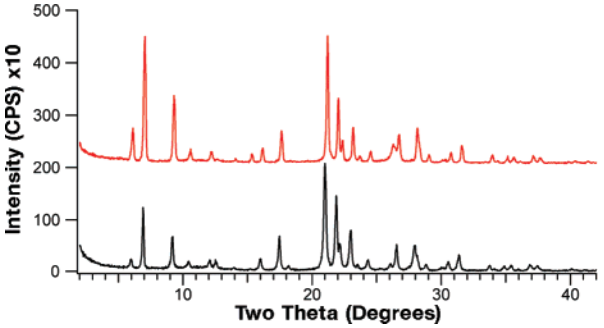

Figure 5. As-made (bottom) and calcined (top) powder XRD (Cu Kα) patterns of borosilicate SSZ-65.

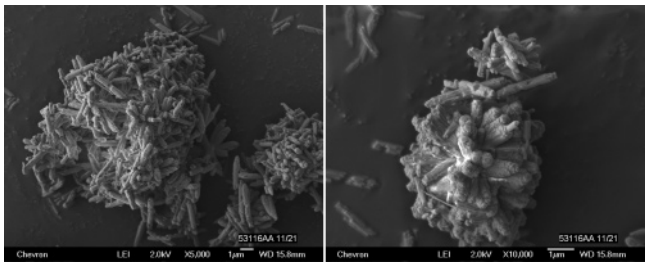

Figure 6. Scanning electron micrographs of crystallites from a borosilicate preparation of SSZ-65.

Results and Discussion

XRD, SEM, HRTEM, and Electron Diffraction Analysis. The XRD peaks for a calcined sample of borosilicate SSZ-65 were indexed in a hexagonal unit cell: a = 16.797 Å, c = 12.618 Å. There were no systematic absences, so the highest possible symmetry could be narrowed to *P*6/*mmm* (191). The XRD patterns of both the as-made and calcined samples (Figure 5) can be indexed in a similar hexagonal unit cell. SEM micrographs (Figure 6) of the borosilicate product showed a morphology of intergrown bundles of segmented, rodlike crystals that are about 0.5 μm in length and 0.1 μm in thickness. A similar morphology is observed in the aluminosilicate preparations; however, there are also a few discrete hexagonal prisms, an observation that is consistent with the crystal symmetry. Electron diffraction (ED) and imaging data obtained using TEM also support the proposed cell. Figure 7A−D shows HRTEM images and corresponding ED patterns along the [100] and [001] projections of SSZ-65. In particular, Figure 7, parts C and D, shows the 6-fold symmetry of the unit cell. The high-resolution images were collected on needle or rodlike crystals that were approximately 0.6−0.8 μm in length and 0.2 μm in width. Strong 12.6 Å fringes were observed perpendicular to the length of the length of the crystals, and 14.9 Å fringes

(40) Chen, C. Y.; Zones, S. I. *Zeolites and Mesoporous Materials at the Dawn of the 21st Century*; Proceedings of the 13th International Zeolite Conference, Montpellier, France, 2001; Studies in Surface Science and Catalysis 135; Galarneau, A., Di Renzo, F., Fujula, F., Vedrine, J., Eds.; Elsevier: Amsterdam, 2001; paper 11-P-16 on CD-ROM.
(41) Larson, A. C.; Von Dreele, R. B. *GSAS The General Structure Analysis System*; Los Alamos National Laboratory: Los Alamos, NM, 1994.
(42) Grosse-Kunstleve, R. W.; McCusker, L. B.; Baerlocher, C. *J. Appl. Crystallogr.* **1997**, *30*, 985.
(43) Baerlocher, C.; Hepp, A.; Meier, W. M. *DLS−76*; ETH: Zurich, Switzerland, 1977.
(44) Lippens, B. C.; Boer, J. H. D. *J. Catal.* **1965**, *4*, 319.

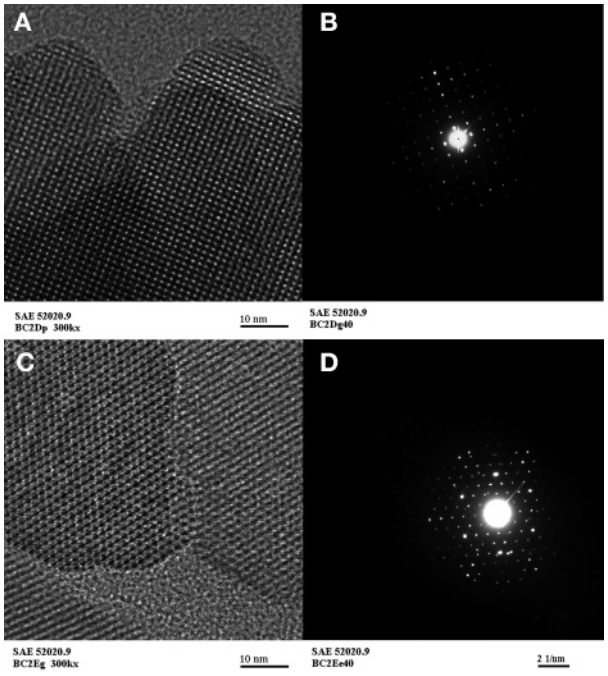

Figure 7. (A) HRTEM image and (B) electron diffraction image of SSZ-65 along [100]; (C) HRTEM image and (D) electron diffraction image of SSZ-65 along [001].

were observed parallel to the needle length. These lattice spacings are apparent in the HRTEM and the zone axis ED images of Figure 7, parts A and B, respectively. In order to obtain a view along the length of the crystals, it was necessary to use a TEM sample prepared by ultramicrotomy. The zone axis pattern (Figure 7D) showed hexagonal symmetry with *d*-spacings of about 14.5 Å.

Structure Solution and Rietveld Refinement. Figure 8 shows the topological model (with oxygen atoms removed) of SSZ-65 determined from the FOCUS algorithm. In space group *P*6/*mmm*, this structure possesses 54 tetrahedral (T) atoms per unit cell and 4 unique T atoms in its asymmetric unit. The coordinates of the DLS-refined structure were used as the starting model for the subsequent Rietveld refinement of the calcined borosilicate sample. The approximate unit cell composition of this particular sample of SSZ-65 is $[Si_{52.5}B_{1.5}O_{108}]$.

For the Rietveld refinement of the synchrotron powder data, soft restraints were placed on the T−O distances (1.60 ± 0.03 Å) and the O−O distances (2.61 ± 0.03 Å). All T atoms were constrained to have the same isotropic thermal factors, and all O atoms were constrained to have the same isotropic thermal factors. In space group *P*6/*mmm* the agreement between the experimental and simulated diffraction pattern was not good for data above 20° 2θ. The R_{wp} and R_p values were 11.58% and 9.40%, respectively, and the $R(F^2)$ value was 0.142. Furthermore, some of the bond distances and bond angles were not close to those anticipated for an ideal SiO_2 structure. The poor agreement may not be a surprise because in this symmetry there are several atoms that lie on high-symmetry positions. We then focused our efforts on space groups of lower symmetry that lack a mirror plane perpendicular to the *z*-axis. However, little or no improvements were observed with these symmetries. In the Fourier difference maps the highest residual electron density (0.7 e/Å^3) was concentrated around atoms Si2 and Si3 (in space group *P*6/*mmm*). Both of these atoms reside on mirror planes parallel to the *z*-axis. This hinted that the symmetry of SSZ-65 might be more accurately described by a space group that lacks these mirror planes. We therefore repeated the refinement in *P*6/*m*. In this space group, the R_{wp}, R_p, and $R(F^2)$ values were 10.28%, 8.51%, and 0.092. The visual agreement above 20° 2θ was also improved. At the completion of the refinement, no electron density above 0.7 e/Å^3 could be found in the Fourier difference maps. Table 1S in the Supporting Information summarizes the details of the data collection and structure refinement, and Table 1 shows the refined atomic coordinates of the structure.

Figure 9 shows the experimental, simulated, and difference profiles for the refinement of the synchrotron powder XRD data. Tables 2S and 3S in the Supporting Information show the T−O bond lengths, the T−O−T bond angles, and the O−T−O bond angles. The tetrahedral angles range from 115.4° to 104.4°, and the average tetrahedral angle is 109.4° for each T site. Two of the unique T sites (12 and 12 per unit cell) have average bond lengths of 1.576 and 1.581 Å. The shortening of the bonds compared to typical Si−O bond lengths (1.60 Å) may be due to the presence of boron. However, if we assume the expected average bond length to be a weighted average of typical tetrahedral B−O and Si−O bond lengths, then this shortening is disproportionate to the boron content (Si/B = 36) within the structure. In structure refinements of certain borosilicate zeolites, we have observed that the average T−O bond lengths are slightly lower than expected. For example, in independently performed structure analyses of powder diffraction data[35] and unpublished single-crystal diffraction data of SSZ-58, we observe ⟨T−O⟩ of 1.58 Å. This suggests there may be secondary effects on the Si−O bond lengths in some borosilicate materials.

Features of the SSZ-65 Structure. SSZ-65 possesses a two-dimensional system of 12-ring pores (Figure 10a) that intersect to form large cavities that possess threefold symmetry (Figure 10b). The micropore volume of the calcined, unexchanged borosilicate (from the *t*-plot method with nitrogen adsorption data) is 0.19 cm^3/g. After a subsequent ammonium exchange and calcination, the micropore volume decreases slightly to 0.17 cm^3/g. The decrease may be due to the removal of framework boron that occupies space in the zeolite micropores. TGA analysis of the as-made zeolite shows a 3.3% mass loss up to 275 °C that is consistent with the desorption of adsorbed water molecules and a 14.1% mass loss between 275 and 625 °C that is consistent with the removal of the occluded organic molecules by pyrolysis and oxidation. This mass loss is equivalent to 2.0 SDA molecules/unit cell or 1.0 SDA/large cage. The measured Si/B ratio is 36, and the Na/B ratio is 0.23. The measured C/N/Cl ratio is 16.0:1.0:0.93. This is close to the ideal chemical formula of the SDA molecule, $C_{16}NH_{23}Cl$. The ideal composition of the as-made zeolite is $[C_{16}NH_{23}Cl]_2[Si_{52.5}B_{1.5}O_{108}]$. Figure 4 shows a comparison of the liquid $^1H-^{13}C$ CP spectrum of the iodide salt of the SDA molecule and the $^1H-^{13}C$ CP MAS solid-state NMR spectrum of the as-made form of SSZ-65. The similarity in the chemical shifts

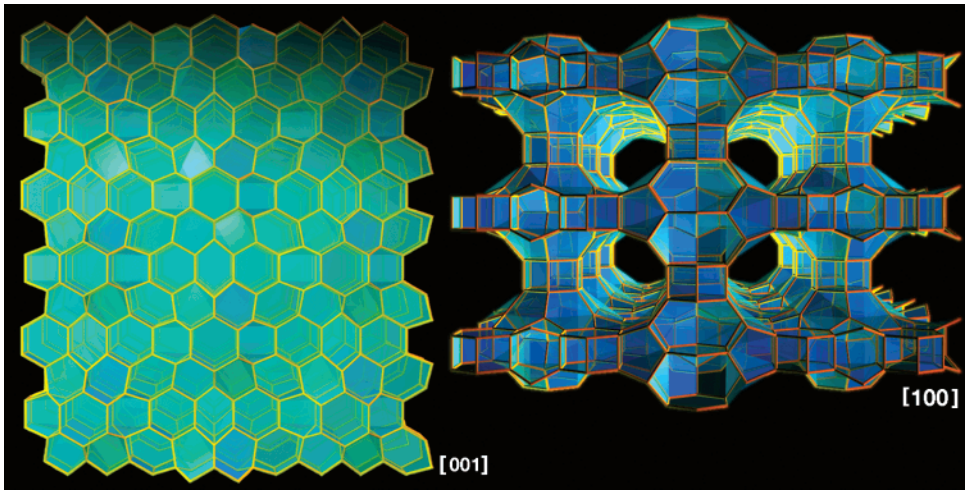

Figure 8. Views of the topological structure of SSZ-65 determined from FOCUS (O atoms omitted).

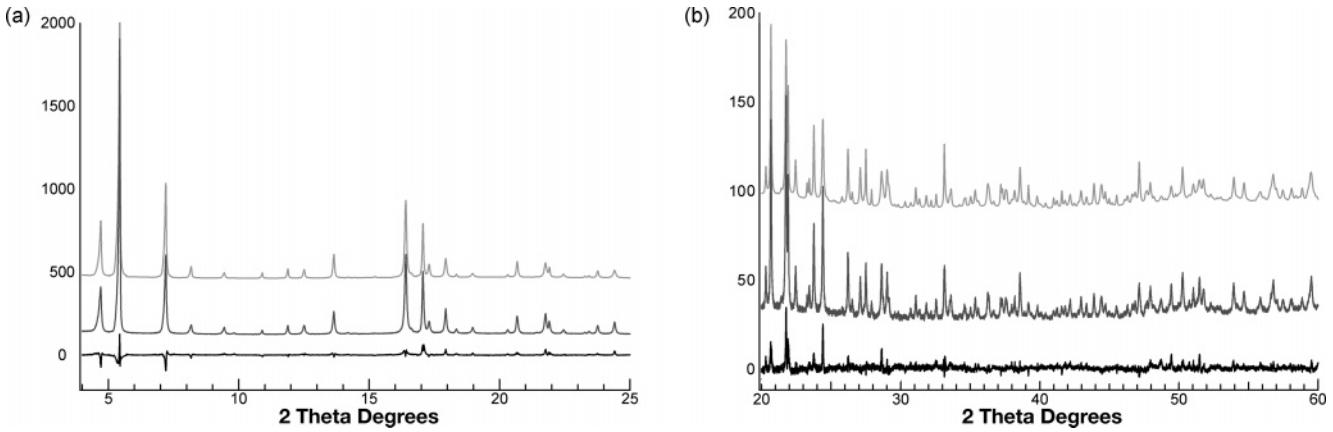

Figure 9. Simulated (top), experimental (middle), and difference (bottom) profiles for the Rietveld refinement of the synchrotron powder diffraction (λ = 1.19958 Å) of a borosilicate sample of SSZ-65 in space group *P*6/*m*: (a) from 4 to 25° 2θ; (b) from 20 to 60° 2θ.

Table 1. Refined Atomic Parameters of Borosilicate SSZ-65 in Space Group *P*6/*m* (175); *a* = 16.8009(2) Å, *c* = 12.6154(1) Å

atom	*x*	*y*	*z*
Si1	0.3017(4)	−0.0029(6)	0.2005(4)
Si2	0.1826(4)	−0.0079(4)	0.3786(4)
Si3	0.1791(7)	−0.0118(9)	0
Si4	0.4991(5)	0.3539(4)	0.1264(5)
Si5	0.4785(5)	0.1606(5)	0.1241(5)
O1	0.3848(5)	0.0967(6)	0.1852(9)
O2	0.3385(6)	0.9271(5)	0.1868(7)
O3	0.2542(6)	−0.0157(9)	0.3083(6)
O4	0.2314(7)	−0.0193(9)	0.1004(5)
O5	0.1782(5)	0.0840(6)	0.3564(6)
O6	0.2100(11)	−0.0149(14)	0.5000
O7	0.1715(10)	0.0789(12)	0
O8	0.4972(11)	0.3657(9)	0
O9	0.4592(11)	0.1421(11)	0
O10	0.5589(6)	0.1456(6)	0.1694(7)
O11	0.5053(5)	0.2645(5)	0.1516(7)

of each spectra and the chemical analysis of the organic elements indicate that the SDA has been occluded intact within the void space of the zeolite structure. The pores are bounded by 12-rings with free diameters of 6.9 Å × 5.9 Å assuming an oxygen radius of 1.35 Å. The structure of SSZ-65 possesses columns (Figure 11a) composed of two consecutive 6^8 cages followed by a 6^24^6 cage, or double six-ring D6R (the descriptor x^ny^m indicates a polyhedral cage with n *x*-rings and m *y*-rings). A similar structural motif occurs in other zeolites that possess a unit cell repeat of 12.4−12.8 Å along the axes of these columns. This motif may be considered as two consecutive n^26^n cages that are connected to an n^24^n cage to form a columnar unit. In SSZ-58 n = 5 (Figure 11b), and in zeolites ITQ-22,[24] ITQ-24,[45] ITQ-13,[23] ITQ-7,[46] and ITQ-17[47] (BEC) n = 4 (Figure 11c).

The framework of SSZ-65 possesses a high density of even-numbered rings. In projection, the layers along [001] are similar to the six-ring sheets observed in cristobalite. In cristobalite the sheets are composed of a single layer of interconnected six-rings in which there is an alternating up−down arrangement of silicon atoms. These are connected to symmetrically equivalent sheets to from the three-dimensional structure. This structural motif is similar to the proposed structure of a silica membrane recently reported by Stacchiola et al.[48] However, it must be noted that although the projections are similar, the up−down arrangements of the tetrahedral atoms are disparate, and the layers in SSZ-65 cannot be neatly defined by sheets that are a single tetrahedral atom in thickness. There are D6R located both

(45) Castaneda, R.; Corma, A.; Fornes, V.; Rey, F.; Rius, J. *J. Am. Chem. Soc.* **2003**, *125* (26), 7820.
(46) Villaescusa, L.; Barrett, P.; Camblor, M. *Angew. Chem., Int. Ed.* **1999**, *38* (13−14), 1997−2000.
(47) Corma, A.; Navarro, M.; Rey, F.; Rius, J.; Valencia, S. *Angew. Chem., Int. Ed.* **2001**, *40* (12), 2277−80.
(48) Stacchiola, D.; Kaya, S.; Weissenrieder, J. *Angew. Chem., Int. Ed.* **2006**, *45* (45), 7636−7639.

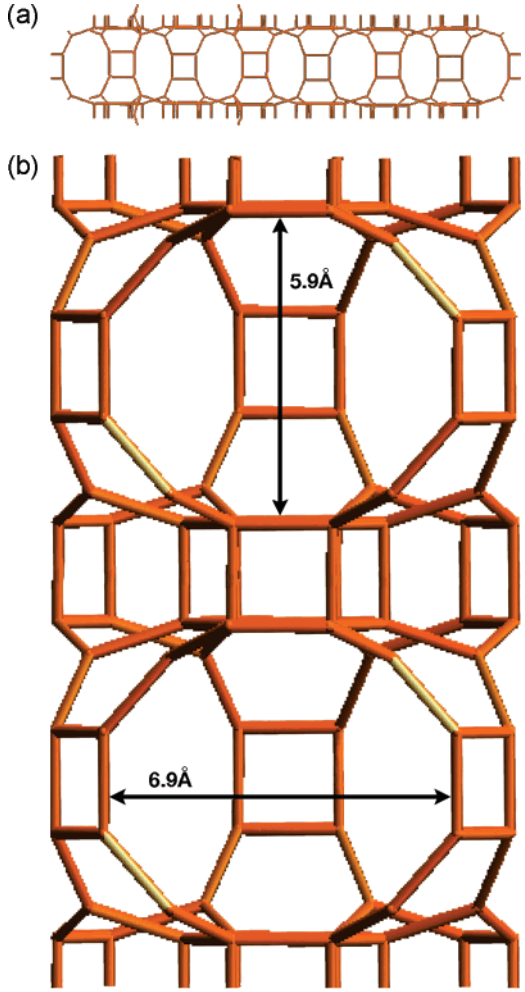

Figure 10. (a) View perpendicular to one 12-ring channel (along [110]) of SSZ 65. (b) View of large cavities (along [1−10]) of SSZ-65.

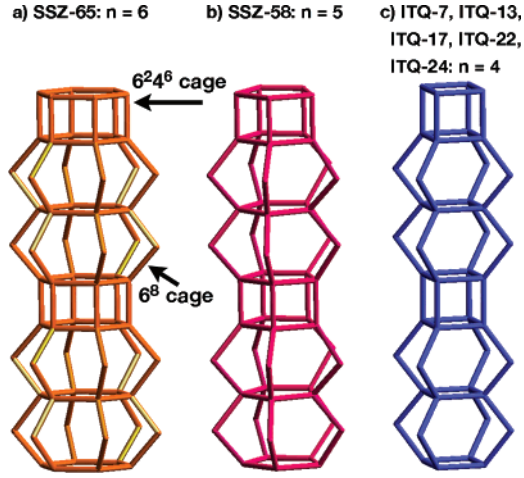

Figure 11. View of the units that link to form columns in (a) SSZ-65, (b) SSZ-58, and (c) ITQ-7, ITQ-13, ITQ-17, ITQ-22, and ITQ-24.

between and within the honeycomb-like layers (Figure 8) that separate the large cages along the *c*-direction. In the past, it was highly unusual from hydroxide-mediated syntheses to prepare high-silica zeolites with a high density of even-numbered rings. Because highly aluminous zeolites possess mostly (or even exclusively) even-numbered rings, it was postulated that this was due to a tendency of aluminum to promote formation of subunits with four-rings.[49] However, of late several high-silica (Si/Al, B > 8) zeolites have been prepared that possess a significant density of four-rings in their structures. These zeolites include SSZ-13 (**CHA**), SSZ-16 (**AFX**),[21] SSZ-24 (**AFI**),[50] SSZ-40 (**AST**), SSZ-55 (**ATS**),[51] MCM-61 (**MSO**),[52] MCM-68 (**MSE**),[53] SSZ-58 (**SFG**), and now SSZ-65. Also, in fluoride-mediated syntheses of all-silica materials, structures with even-numbered rings are frequently observed. We have recently discussed how zeolites with aluminum, boron, or framework-bound fluoride are better able to accommodate a higher density of extraframework charge than all-silica zeolites because of destabilizing effects that siloxy/silanol defects have on framework energies.[49] Open framework structures tend to have small building units comprised of a large number of four-rings (or three-rings in structures with framework lithium,[54] beryllium,[55] or zinc[56,57]). In any case, it is no longer exceptional to observe high-silica zeolites that have a large proportion of four-rings.

Databases of Hypothetical Zeolite Structures. Recent work has been done to provide databases of hypothetical zeolite structures to the general community.[58] To date, the development of these databases has been restricted to a limited number of space groups of high symmetry and to a limited number of T atoms per asymmetric unit. A practical measure of these databases is their ability to predict the structures of previously unreported materials that possess the appropriate symmetries and number of unique T atoms. *P6/mmm* is one of the space groups that has been examined by both Treacy and co-workers[59,60] and by Earl and Deem.[61] The databases of Treacy and Deem both possess the framework of SSZ-65.

Conclusions

SSZ-65 is a new zeolite that can be prepared either as a borosilicate or as an aluminosilicate using 1-ethyl-1-(1-(4-chlorophenyl)-cyclopropylmethyl)-pyrrolidinium as an SDA. The aluminosilicate form of SSZ-65 may be prepared by using zeolite Y as an aluminum source or by performing a postsynthetic treatment of the borosilicate with a solution of aluminum nitrate. The powder diffraction patterns of the as-made and calcined forms of SSZ-65 can be indexed in a

(49) Burton, A. W.; Zones, S. I.; Elomari, S. *Curr. Opin. Colloid Interface Sci.* **2005**, *10*, 211−219.
(50) Bialek, R.; Meier, W. M.; Davis, M.; Annen, M. J. *Zeolites* **1991**, *11*, 438−442.
(51) Wu, M. G.; Deem, M. W.; Elomari, S. A.; Medrud, R. C.; Zones, S. I.; Maesen, T.; Kibby, C.; Chen, C.-Y.; Chan, I. Y. *J. Phys. Chem. B* **2002**, *106*, 264−270.
(52) Shantz, D. F.; Burton, A.; Lobo, R. F. *Microporous Mesoporous Mater.* **1999**, *31*, 61−73.
(53) Dorset, D. L.; Weston, S. C.; Dhingra, S. S. *J. Phys. Chem. B* **2006**, *110*, 2045−2050.
(54) Park, S. H.; Daniels, P.; Gies, H. *Microporous Mesoporous Mater.* **2000**, *37* (1), 129−143.
(55) Cheetham, A. K.; Fjellvåg, H.; Gier, T. E.; Kongshaug, K. O.; Lillerud, K. P.; Stucky, G. D. *Stud. Surf. Sci. Catal.* **2001**, *135*, 158.
(56) Annen, M. J.; Davis, M. E.; Higgins, J. B.; Schlenker, J. L. *Chem. Commun.* **1991**, 1175−1176.
(57) Röhrig, C.; Gies, H. *Angew. Chem., Int. Ed.* **1995**, *34*, 63−65.
(58) Foster, M. D.; Treacy, M. M. J. *Atlas of Prospective Zeolite Frameworks.* http://www.hypotheticalzeolites.net/ (accessed March 21, 2007).
(59) Treacy, M. M. J.; Randall, K. H.; Rao, S.; Perry, J. A.; Chadi, D. J. *Z. Kristallogr.* **1997**, *212*, 768−791.
(60) Treacy, M. M. J.; Rivin, I.; Balkovsky, E.; Randall, K. H.; Foster, M. D. *Microporous Mesoporous Mater.* **2004**, *74*, 121−132.
(61) Earl, D. J.; Deem, M. W. *Ind. Eng. Chem. Res.* **2006**, *45*, 5449−5454.

hexagonal unit cell. The highest topological symmetry of SSZ-65 is *P*6/*mmm*. However, improvement in the Rietveld refinement is obtained in space group *P*6/*m*.

SSZ-65 has a two-dimensional system of 12-ring pores that intersect to form large cavities. The framework of SSZ-65 possesses a large density of double six-ring (D6R) units that are quite unusual in high-silica zeolite materials. SSZ-65 is another example of a high-silica material with a large proportion of even-numbered rings in its framework. The unit cell dimension of 12.6 Å is characteristic of the repeat distance of columnar units composed of two consecutive $n^2 6^n$ cages followed by an $n^2 4^n$ cage. This structural motif should therefore be considered in unsolved zeotype structures that possess this unit cell dimension.

Acknowledgment. We thank Steve Trumbull for assistance with the zeolite syntheses and Tom Rea for collection of the SEM data. We also thank Stacey Zones for useful discussion. This work was supported by the Chevron Energy Technology Company. We are grateful to G. L. Scheuerman and C. R. Wilson for support of the new materials research program at Chevron. We also acknowledge the assistance of Jae-Hyuk Her and Peter Stephens in the collection of the synchrotron diffraction data. Research was carried out in part at the National Synchrotron Light Source, Brookhaven National Laboratory, which is supported by the U.S. Department of Energy, Division of Materials Sciences and Division of Chemical Sciences.

Supporting Information Available: Fractional coordinates of SSZ-65 in highest topological symmetry (Table 1S), atomic distances and Si−O−Si angles of SSZ-65 framework atoms (Table 2S), tetrahedral angles of framework atoms in SSZ-65 (Table 3S), experimental and refinement parameters of synchrotron powder X-ray diffraction experiment for SSZ-65 (Table 4S), the simulated, experimental, and difference profiles for the Rietveld refinement of the synchrotron powder diffraction of a borosilicate sample of SSZ-65 in space group *P*6/*mmm* (Figures 1S and 2S), comparison of the difference plots for the Rietveld refinements of SSZ-65 in the space groups *P*6/*m* and *P*6/*mmm* (Figure 3S) (PDF). This material is available free of charge via the Internet at http://pubs.acs.org.

CM070459T